

Metabolomic signatures of chronic kidney disease of diverse etiologies in the rats and humans

Zhi-Hao Zhang, Hua Chen, Nosratola D. Vaziri, Jia-Rong Miao, Li Zhang, Xu Bai, and Ying-Yong Zhao

J. Proteome Res., **Just Accepted Manuscript** • DOI: 10.1021/acs.jproteome.6b00583 • Publication Date (Web): 16 Sep 2016

Downloaded from <http://pubs.acs.org> on September 19, 2016

Just Accepted

“Just Accepted” manuscripts have been peer-reviewed and accepted for publication. They are posted online prior to technical editing, formatting for publication and author proofing. The American Chemical Society provides “Just Accepted” as a free service to the research community to expedite the dissemination of scientific material as soon as possible after acceptance. “Just Accepted” manuscripts appear in full in PDF format accompanied by an HTML abstract. “Just Accepted” manuscripts have been fully peer reviewed, but should not be considered the official version of record. They are accessible to all readers and citable by the Digital Object Identifier (DOI®). “Just Accepted” is an optional service offered to authors. Therefore, the “Just Accepted” Web site may not include all articles that will be published in the journal. After a manuscript is technically edited and formatted, it will be removed from the “Just Accepted” Web site and published as an ASAP article. Note that technical editing may introduce minor changes to the manuscript text and/or graphics which could affect content, and all legal disclaimers and ethical guidelines that apply to the journal pertain. ACS cannot be held responsible for errors or consequences arising from the use of information contained in these “Just Accepted” manuscripts.

Metabolomic signatures of chronic kidney disease of diverse etiologies in the rats and humans

Zhi-Hao Zhang³, Hua Chen¹, Nosratola D. Vaziri², Jia-Rong Miao⁴, Li Zhang⁵, Xu Bai⁶, Ying-Yong Zhao^{1,2,*}

¹Key Laboratory of Resource Biology and Biotechnology in Western China, Ministry of Education, the College of Life Sciences, Northwest University, No. 229 Taibai North Road, Xi'an, Shaanxi 710069, China

²Division of Nephrology and Hypertension, School of Medicine, University of California Irvine, MedSci 1, C352, UCI Campus, Irvine, California, 92897, USA

³BioEnergy Science Center and Biosciences Division, Oak Ridge National Laboratory, Oak Ridge, TN 37831, USA

⁴Department of Nephrology, Affiliated Hospital of Shaanxi Institute of Traditional Chinese Medicine, No. 2 Xihuamen, Xi'an, Shaanxi 710003, China

⁵Department of Nephrology, Xi'an No. 4 Hospital, No. 21 Jiefang Road, Xi'an, Shaanxi 710004, China

⁶Solution Centre, Waters Technologies (Shanghai) Ltd., No. 1000 Jinhai Road, Shanghai 201203, China

Corresponding authors:

Ying-Yong Zhao, PhD, MD, Professor

Key Laboratory of Resource Biology and Biotechnology in Western China, Ministry of Education, Northwest University, Xi'an, 710069, China, Tel: +86 29 88305273; Fax: +86 29 88303572; E-mail: zyy@nwu.edu.cn; zhaoyybr@163.com

Abstract

Chronic kidney disease (CKD) has emerged as a major public health problems worldwide. It frequently progresses to end-stage renal disease which is related to very high cost and mortality. Novel biomarkers can provide insight into the novel mechanism, facilitate early detection and monitor progression of CKD and its response to therapeutic interventions. To identify potential biomarkers, we applied an UPLC-HDMS together with univariate and multivariate statistical analyses using plasma samples from patients with CKD of diverse etiologies (100 sera in discovery set and 120 sera in validation set) and two different rat models of CKD. Using comprehensive screening and validation workflow, we identified a panel of seven metabolites which were shared by all patients and animals regardless of the underlying cause of CKD. These included ricinoleic acid, stearic acid, cytosine, LPA(16:0), LPA(18:2), 3-methylhistidine, and argininic acid. The combination of these seven biomarkers enabled the discrimination of patients with CKD from healthy subjects with a sensitivity of 83.3% and a specificity of 96.7%. In addition, these biomarkers accurately reflected improvements in renal function in response to the therapeutic interventions. Our results indicated that the identified biomarkers may improve the diagnosis of CKD and provide a novel tool for monitoring of the progression of disease and response to treatment in CKD patients.

Keywords: chronic kidney disease, adenine-induced CKD rats, 5/6 nephrectomized rats, metabolomics, biomarker, irbesartan, enalapril, plasma

1. Introduction

Chronic kidney disease (CKD) which leads to progressive loss of kidney function has become a primary public health problem involved with 11% of the U.S. population.¹ Individuals with CKD are at high risk for cardiovascular mortality and progression to end-stage renal disease (ESRD).^{2,3} One of the major hurdles toward improving clinical outcome of CKD has been the lack of diagnostic biomarkers at early stages of the disease. Current clinical and laboratory methods for CKD diagnosis are limited to measurement of plasma urea and creatinine, urinary protein excretion, and measurement of creatinine clearance or the estimated glomerular filtration rate (eGFR). However, all of these methods are problematic to some extent. Serum creatinine is not an adequately sensitive marker for the early detection of kidney damage since it is affected by age, race, gender, muscle mass, total body weight and nutritional status. While being useful in mass screening for CKD, proteinuria and the decline in eGFR are relatively insensitive markers and have limited value in the detection of early phases of kidney injury.⁴ Hence, more sensitive and cost-effective biomarkers are needed to identify the at-risk patients earlier in the disease process and to carefully monitor progression of CKD and its response to treatment in this vulnerable population.

Emerging platforms in the biomedical arena offer a new tool to identify novel biomarkers. Metabolomics is a new member of omics technologies that focuses on either qualitative or quantitative measurement of the dynamic multi-parametric metabolic response of living organisms to pathophysiological stimuli. It is rapidly emerging as a discovery tool for identification of the new diagnostic and prognostic biomarkers of human diseases.⁵⁻⁷ Our previous studies have shown the usefulness of UPLC-HDMS-based metabolomics approach for diagnosis and evaluation of CKD.⁸⁻¹⁰ We have found a series of metabolites which are significantly altered in CKD, reflecting metabolic dysfunction in the pathway of glycerophospholipid, fatty acid, amino acid, purine, taurine and choline metabolisms. However, no individual metabolites or combination of metabolites have been evaluated for their value as biomarkers for diagnosis and monitoring of the CKD progression and its response to therapeutic

1
2 interventions.

3
4 The most widely used animal models of CKD are 5/6 nephrectomized rats and rats with the adenine-induced
5
6 nephropathy. 5/6 nephrectomy leads to progressive glomerular sclerosis while the adenine exposure results in
7
8 tubulointerstitial nephropathy with crystal precipitation.¹¹ The situation of patients with CKD is much more
9
10 complex: patients may have either renal glomerular or tubular lesions or both. Thus, in present study, the
11
12 UPLC/HDMS-based metabolomics was applied to plasma samples from rats with adenine-induced CKD, rats with
13
14 5/6 nephrectomized CKD and patients with diverse forms of CKD (50 controls and 50 CKD patients) to identify
15
16 common and reliable plasma biomarkers for CKD of diverse etiologies and to gain in depth insight into the
17
18 CKD-related metabolic changes. To this end in our study we compared the differentially metabolites among the
19
20 two animal models and patients with CKD and then selected biomarkers from these metabolites which appeared in
21
22 both patients as well as the two different model of CKD in rats. To enhance the accuracy and applicability of the
23
24 potential biomarkers to the clinical setting, we designed and employed a two-step verification strategy to verify
25
26 the potential biomarkers. An overview of the study design is shown in Figure 1.
27
28
29
30
31
32
33
34

35 **2. Materials and Methods**

36 **2.1. Chemicals**

37
38 Creatinine and adenine were purchased from the National Institutes for Food and Drug Control and Sigma
39
40 Chemical Co., Ltd. All the antibodies were from Abcam Company or Santa Cruz Biotechnology.
41
42
43
44

45 **2.2. Human samples**

46
47 Plasma samples (clinical and demographic summary in Table 1) were provided by the Affiliated Hospital of
48
49 Shanxi Institute of Traditional Chinese Medicine and Xi'an No. 4 Hospital, Xi'an, China. The study was approved
50
51 by the ethics committee of the involved institutions. Written informed consent was obtained from each participant
52
53 before their inclusion in the study. Plasma from a total of 100 individuals including 50 controls and 50 CKD
54
55 stages 4–5 patients was collected for the further analysis. Plasma from another set of 120 individuals including 30
56
57
58
59
60

4

1
2 controls, 30 CKD stages 4–5 patients, 30 CKD patients with enalapril treatment and 30 CKD patients with
3
4 irbesartan treatment was collected for the validation of biomarkers. CKD+enalapril and CKD+irbesartan patients
5
6 were orally administered enalapril (10 mg/day) and irbesartan (150 mg/day) for 8 weeks. CKD stages 4–5 were
7
8 defined as eGFR < 29 ml/min/1.73 m², MDRD-4 equation. We will refer to ‘CKD stages 4–5’ as ‘CKD’ all along
9
10 the manuscript. Plasma was collected and stored at –80 °C until analysis.
11
12

13 14 **2.3. Animal experiments.**

15 16 **2.3.1. Adenine-induced CKD model**

17
18 Male Sprague-Dawley rats, weighing 200 ± 10 g were purchased from Fourth Military Medical University (Xi’an,
19
20 China). The rats were randomly to divide into the following four groups (n=8): control, CKD, CKD+irbesartan
21
22 and CKD+ergone groups. CKD, CKD+irbesartan and CKD+ergone groups received adenine dissolved in 1% (w/v)
23
24 gum acacia solution (200 mg/kg body weight) by oral gavage once every day for three weeks.^{8, 12} Control group
25
26 received the same volume of gum acacia solution. CKD+irbesartan and CKD+ergone groups were orally
27
28 administered irbesartan (20 mg/kg/day) and ergone (20 mg/kg/day) for six weeks starting 3 hours after adenine
29
30 gastric gavage. All the rats were anesthetized with 10% urethane and plasma samples were collected by carotid
31
32 artery cannula at week 6. Plasma was collected and stored at –80 °C until analysis. This study was approved by
33
34 the Ethical Committee of Northwest University and studies were conducted in accordance with the Chinese
35
36 national legislation and local guidelines.
37
38
39
40
41
42
43
44

45 46 **2.3.2. 5/6 nephrectomy CKD model**

47
48 Male Sprague-Dawley rats (225–250 g) were fed regular rat chow and water ad libitum and randomly assigned to
49
50 the control, CKD, CKD+enalapril and CKD+ RTA dh404 groups (n=8). The animals allocated to the CKD,
51
52 CKD+enalapril and CKD+ RTA dh404 groups underwent 5/6 nephrectomy by surgical resection of the upper and
53
54 lower thirds of left kidney, as described previously.¹³ The animals allocated to the control group underwent sham
55
56 operation. CKD+enalapril and CKD+ RTA dh404 groups were orally administered enalapril (10 mg/kg/day) and
57
58
59
60

1
2 RTA dh404 (2 mg/kg/day) for 12 weeks starting immediately prior to surgery. The procedures were carried out
3
4 under general anesthesia (50 mg/kg ip Nembutal) using strict hemostasis and aseptic techniques. All the rats were
5
6 anesthetized with 10% urethane, and plasma samples were obtained by carotid artery cannula at week 12. Plasma
7
8 was collected and stored at -80°C until analysis.
9
10

11 12 **2.4. Biochemical determination**

13
14 Serum and urine biochemistry were analyzed as described in detail previously.¹⁴ The measurements for each of the
15
16 samples for biochemical parameters were replicated 3 times.
17
18

19 20 **2.5. Renal histology and immunohistochemistry**

21
22 H&E, PAS, Masson trichrome staining, TGF- β 1, ED-1, PCNA and iNOS immunohistochemical staining were
23
24 performed according to published methods.^{9, 10, 15} The materials and methods of this section was described in
25
26 detail in supplementary materials. The measurements for each of the samples were replicated 3 times.
27
28

29 30 **2.6. Metabolomics**

31
32 Plasma for metabolomics was prepared as described previously.¹⁴ Metabolomics were performed on a Waters
33
34 AcquityTM Ultra Performance LC system equipped with a Waters XevoTM G2-S QToF MS. Chromatographic
35
36 separation, mass spectrometry, data processing were described in the Supporting information.
37
38

39 40 **2.7. Statistics**

41
42 Fold changes from CKD group/control group and ROC curve was performed by Metaboanalysis 3.0. Differences
43
44 between the means of the two groups were analyzed using Student's t-test and Mann-Whitney test by SPSS 19.0.
45
46 VIP was used to rank the contribution of each variable based on the PLS-DA model, and those variables with $\text{VIP} >$
47
48 1.0 are considered relevant for group discrimination.¹⁶ The critical p-value was set at 0.05 for this study. Based on
49
50 the Hochberg-Benjamini method, the resultant p values from Student's t-test were further adjusted by an FDR.
51
52
53

54 55 **3. Results**

56 57 **3.1. General data**

58
59
60
6

1
2 The CKD patients exhibited hypertension, proteinuria, significant increase in plasma urea, creatinine, uric acid,
3
4 and triglyceride concentrations, and significant reductions in serum albumin, red blood cell count and blood
5
6 hemoglobin concentrations (Table 1). Compared with the control group, rats in both CKD models exhibited
7
8 significantly increased creatinine, urea, triglycerides and total cholesterol concentrations and significant reduction
9
10 in creatinine clearance (Ccr) (Table 2). As expected the 5/6 nephrectomized CKD rats showed significantly greater
11
12 proteinuria and hyperlipidemia when compared with the CKD rats with adenine-induced chronic tubulointerstitial
13
14 nephropathy. Physiologic parameters of animals showed in Table 3.
15
16
17
18
19

20 **3.2. Metabolomics data**

21
22 Validation of UPLC-HDMS findings is described in detail in the Supplementary information. Metabolic profiling
23
24 of plasma sample including CKD patients, adenine-induced CKD rats, and 5/6 nephrectomized rats was acquired
25
26 using UPLC-HDMS in ESI⁺ and ESI⁻ modes. Since metabolites detected in both ESI⁺ and ESI⁻ modes
27
28 complemented each other, data generated from ESI⁺ and ESI⁻ modes were combined to perform statistical
29
30 analysis. As shown in Figure S1, principal component analysis (PCA) and the partial least-square-discriminant
31
32 analysis (PLS-DA) showed a clear intergroup separation in plasma metabolites from control group and CKD
33
34 patients and between control rats and rats with adenine-induced CKD. For 5/6 nephrectomized rats, PCA showed
35
36 a trend for intergroup separation and PLS-DA displayed a clear separation between control and CKD groups
37
38 (Figure S1). The PCA and PLS-DA results indicated significant alteration in plasma metabolic profiles in patients
39
40 with CKD and rats with CKD of distinctly different etiologies. Differential metabolites contributing to the altered
41
42 metabolic profiles of patients with CKD and rats with adenine-induced CKD and 5/6 nephrectomized CKD were
43
44 identified according to the previously reported methods^{17, 18} and summarized in Tables S1, S2 and S3 respectively.
45
46
47 They were selected using the VIP (variable importance in the projection) values (>1.0) combined with Student's
48
49 t-test ($p < 0.05$) with a false discovery rate (FDR) < 0.05 and Mann-Whitney U test ($p < 0.05$).
50
51
52
53
54
55
56
57

58 We identified 71, 96 and 43 differential metabolites from patients with CKD, 5/6 nephrectomized CKD rats,
59
60

1
2 and adenine-induced CKD rats respectively (Tables S1-S3). We then applied heatmap based on the analysis of
3
4 Pearson correlation coefficients to visualize the relative levels of the differential metabolites (Figure S2). As
5
6 shown in Figure 2A, 26 metabolites showed similar trends in the CKD patients and 5/6 nephrectomized CKD rats;
7
8 13 metabolites showed similar trends in CKD patients and adenine-induced CKD rats and 3 metabolites showed
9
10 similar trends in CKD patients with both CKD animal models. Thus, these 36 differential metabolites ($p < 0.05$)
11
12 were selected as biomarker candidates of CKD. The distribution of these 36 metabolites across all specimens from
13
14 CKD patients is presented in the z-score plots (Figure 2B). The heatmap of these 36 candidate biomarkers is
15
16 shown in Figure 2C.
17
18
19
20
21

22 The significance analysis of microarrays (SAM) was used to select the most significant metabolites (Figure
23
24 S3). A total of 17 metabolites, which were the most significant metabolites for the differentiation of the CKD from
25
26 the control groups were retained in the candidate pool (Table 4). Subsequently, the diagnostic potential of these
27
28 candidates was evaluated. Receiver operating characteristic (ROC) curve was exploited based on the results of the
29
30 area under the curve (AUC), the sensitivity, and specificity at the best cutoff points (Figure 2D). Table 4 shows the
31
32 results of ROC analysis for the discovery set. As shown in Table 4, 3-hydroxyhexadecanoic acid, MG(15:0),
33
34 lipoyllysine, arachidic acid, creatinine, tryptophanol and docosapentaenoic acid were removed from the candidate
35
36 pool because of the low AUC, sensitivity or specificity. Thus, a total of 10 metabolites were retained in the
37
38 candidate pool. Figure 3 presents the relative contents of these 10 potential biomarkers across all groups. The
39
40 concentrations of 12-ketodeoxycholic acid and indolelactic acid were significantly increased in CKD patients
41
42 compared to control group but were significantly decreased in 5/6 nephrectomized CKD rats compared to the
43
44 control rats. Similarly, the concentration of hypotaurine was significantly decreased in CKD patients compared to
45
46 the control group but was significantly increased in rats with adenine-induced CKD compared to the control rats.
47
48 Therefore these three candidate biomarkers presented opposite trends on the effect of CKD in patients and rats and
49
50 were removed from the candidate pool.
51
52
53
54
55
56
57
58
59
60

1
2
3 Finally, hierarchical cluster analysis (HCA) was performed to reveal the correlation among the remaining
4
5 seven candidates. These candidates were clustered into two groups in the light of their Pearson correlation
6
7 coefficients (Figure. 3A, I–II). Cluster I included two fatty acids (ricinoleic acid and stearic acid) and cytosine.
8
9 Cluster II consisted of two lipids [LPA(16:0) and LPA(18:2)], 3-methylhistidine and argininic acid.
10
11

12 **3.3. Validation of Metabolic Biomarkers**

13 **3.3.1. The first step verification**

14
15
16
17 Another independent set of plasma samples (30 patients and 30 healthy subjects) was collected and analyzed in
18
19 the validation phase to validate the reliability of these seven candidates as biomarkers of CKD. As shown in
20
21 Figure 4B, twenty-five out of thirty CKD patients were correctly grouped (83.3% sensitivity). Twenty-nine out of
22
23 thirty healthy individuals were correctly grouped (96.7% specificity). Figure 4C and 4D shows the ROC curves of
24
25 thirty healthy individuals were correctly grouped (96.7% specificity). Figure 4C and 4D shows the ROC curves of
26
27 the individual biomarkers and the combination of the 7 biomarkers from CKD patients in validation phase.
28
29

30 **3.3.2. The second step verification**

31
32 A number of clinical and experimental animal studies have demonstrated that up-regulation of renin-angiotensin
33
34 system are closely associated with progression of renal disease.^{13, 19} Several clinical trials have shown that
35
36 irbesartan (IRB) significantly slows the progression of diabetic nephropathy and non-diabetic advanced CKD.^{20, 21}
37
38 Ergosta-4,6,8(14),22-tetraen-3-one (ergone) is one of the bioactive steroids from *Cordyceps sinensis*.²² Our
39
40 previous study revealed that ergone were able to prevent progression of renal injury and subsequent renal
41
42 fibrosis.^{23, 24} To further validate the biomarker candidates, we tested whether administration of irbesartan and
43
44 ergone can attenuate tubulointerstitial fibrosis and improve abnormalities of the identified biomarker candidates
45
46 including 3-methylhistidine, argininic acid, LPA(18:2) and cytosine in adenine-induced CKD rats. We treated rats
47
48 with daily administration of irbesartan and ergone 3 hours after daily administration of adenine by gastric gavage
49
50 for six weeks. Treatment with irbesartan and ergone improved renal histology, reduced fibrosis, kidney injury and
51
52 expression of fibrotic proteins (Figure 4E, 4K) and improved renal function (Figure 4F) in CKD rats. In addition,
53
54
55
56
57
58
59
60

1
2 irbesartan significantly decreased upregulation of 3-methylhistidine, argininic acid and partially reversed
3
4 downregulation of cytosine. In addition irbesartan attenuated upregulation of LPA(18:2) however the difference
5
6 did not reach statistical significance (Figure 4G). In contrast to irbesartan, ergone failed to reverse the
7
8 adenine-induced changes of all the candidate biomarkers.
9
10

11
12 Enalapril is an angiotensin-converting-enzyme inhibitor widely used in CKD patients.²⁵ Oxidative stress and
13
14 inflammation play a major role in the development and progression of CKD and are, in part, mediated by the
15
16 impaired activation of the cytoprotective transcription factor, nuclear factor-erythroid-2-related factor 2 (Nrf2).²⁶
17
18 Protective effects of Nrf2 are proved by amelioration of oxidative stress, inflammation, and kidney diseases with
19
20 administration of natural Nrf2 activators in animal models,^{27, 28} and occurrence of autoimmune nephritis in Nrf2
21
22 knock out mice.²⁶ In fact administration of the synthetic triterpenoid RTA dh404
23
24 (2-cyano-3,12-dioxooleana-1,9-dien-28-oic acid-9,11-dihydro-trifluoroethyl amide or CDDO-dhTFEA), a Nrf2
25
26 activator, has been shown to retard CKD progression in 5/6 nephrectomized rats.²⁹
27
28
29
30
31

32
33 Next we examined whether administration of enalapril and RTA dh404 can attenuate CKD progression and
34
35 improve abnormalities of the candidate biomarkers including LPA(16:0), stearic acid, LPA(18:2) and ricinoleic
36
37 acid in 5/6 nephrectomized rats. Rats received Enalapril and RTA dh404 once daily for 12 weeks after 5/6
38
39 nephrectomy. Treatments with enalapril and RTA dh404 reduced interstitial fibrosis, inflammation, kidney injury
40
41 and expression of fibrotic protein (Figure 4H, 4L) and improved renal function (Figure 4I) compared to the
42
43 untreated 5/6 nephrectomized rats. As shown in Figure 4J, enalapril significantly decreased upregulation of
44
45 LPA(16:0), LPA(18:2) and reversed downregulation of stearic acid. Likewise, RTA dh404 significantly decreased
46
47 upregulation of LPA(16:0), LPA(18:2) and reversed downregulation of stearic acid and ricinoleic acid.
48
49
50
51

52
53 Finally, we examined whether administration of enalapril and irbesartan can attenuate CKD progression and
54
55 attenuate the abnormalities of the 7 candidate biomarkers in patients with CKD. Enalapril and irbesartan were
56
57 orally administered once daily for 8 weeks. Enalapril and irbesartan showed similar effects on the abnormal
58
59
60

1
2 candidate biomarkers. They significantly decreased upregulation of LPA(16:0), LPA(18:2), 3-methylhistidine, and
3
4 argininic acid and reversed downregulation of cytosine and ricinoleic acid (Figure 4M).
5
6

7 **4. Discussion**

8
9
10 In the present study, we used UPLC-HDMS-based metabolomic approach to profile plasma metabolites in order
11
12 to identify potential common plasma biomarkers of CKD in rats with adenine-induced CKD and 5/6
13
14 nephrectomized CKD and in patients with CKD. We included samples from different animal models of CKD
15
16 and patients with CKD of diverse etiologies in order to identify the biomarkers of CKD itself by excluding the
17
18 impact of changes caused by the underlying cause of CKD.
19
20
21

22
23 The study was divided into two parts, including discovery and validation (Figure 1). In discovery phase, we
24
25 applied a comprehensive workflow to identify novel biomarkers. In validation phase, we collected and analyzed
26
27 another batch of plasma samples including including 30 controls, 30 CKD patients, 30 CKD patients with
28
29 enalapril treatment and 30 CKD patients with irbesartan treatment to validate the reliability of these seven
30
31 biomarker candidates. We used the same methods of sample pretreatment, instrumental detection, and data
32
33 analysis. These seven biomarkers offered good diagnostic performances for discrimination of patients with CKD
34
35 from healthy subjects with a sensitivity of 83.3%, a specificity of 96.7% (Figure 4B) and a AUC of 0.997 (Figure
36
37 4D). The results indicated that the seven biomarkers could be improved by the irbesartan, ergone, enalapril or RTA
38
39 dh404 treatments (Figure 4G, 4J, 4M). Therefore, collectively these metabolites represented satisfactory
40
41 biomarkers for clinical diagnosis, monitoring of disease progression, and response to therapeutic interventions in
42
43 CKD of diverse etiologies.
44
45
46
47
48
49

50
51 In an attempt to gain a deeper understanding of the identified biomarkers, we performed a systematic
52
53 pathway analysis based on 36 significantly differential metabolites. As shown in Figure 5A, the CKD-associated
54
55 metabolic perturbation involved pathways of glycerophospholipid, taurine, hypotaurine and fatty acid metabolism
56
57 among others. Figure 5B shows the metabolic pathways of identified biomarkers. The present study showed a
58
59
60

1
2 clear increase in plasma 3-methylhistidine and argininic acid in CKD patients. Both of these compounds are
3
4 among uremic toxins which have been implicated in progression of CKD and development of CKD-related
5
6 complications. Earlier study has revealed a significant increase in plasma 3-methylhistidine in patients with stage
7
8 3–4 CKD,³⁰ confirming the results of the present study. In addition, using ¹H-NMR spectroscopy Choi et al³¹
9
10 found significant retention of multiple uremic toxins including 3-methylhistidine in CKD patients maintained on
11
12 dialysis. The decline in renal function invariably results in metabolic acidosis. Graham investigated six chronic
13
14 hemodialysis patients before and after correction of acidosis.³² With the correction of the metabolic acidosis, they
15
16 found the level of 3-methylhistidine was reduced significantly. The latter is considered a valid marker for skeletal
17
18 muscle breakdown in humans. Thus, the marked elevation of plasma 3-methylhistidine reflects accelerated loss of
19
20 muscle mass in patients with CKD. Argininic acid, a guanidine compound, is a urea derivative. Blood level of
21
22 guanidine compounds rise as a result of excess dietary intake or impaired clearance by the kidneys. Blood
23
24 concentration of argininic acid is significantly increased in uremic compared to the normal populations.³³ Our
25
26 previous study demonstrated significant increase in plasma argininic acid in rats with adenine-induced CKD.¹⁰
27
28 These findings are consistent with the result of the present study.
29
30
31
32
33
34
35
36

37 Decreased plasma stearic acid and ricinoleic acid were observed in our patients with CKD. Abnormal fatty
38
39 acid metabolism is closely related to CKD. Recent study show that dysfunction of fatty acid oxidation rather than
40
41 intracellular lipid accumulation induces the development of renal fibrosis.³⁴ Stearic acid has been reported to be
42
43 decreased in the plasma of CKD patients and decreased abundance of stearic acid, was associated with declining
44
45 renal function.³⁵ Ricinoleic acid has been reported to be decreased in the plasma of in rats with adenine-induced
46
47 CRF.¹⁰
48
49
50
51

52 CKD is associated with accumulation of lipids in the renal tissue which is primarily due to tubular
53
54 reabsorption of filtered lipid-bound proteins^{36, 37} and impaired fatty acid oxidation and contributes to the
55
56 pathogenesis of renal fibrosis.³¹ Our CKD patients exhibited significant reduction of plasma stearic acid and
57
58
59
60

1
2 ricinoleic acid levels. These findings are in accord with the results of the earlier studies which have shown
3
4 reduced plasma stearic acid in CKD patients³² and reduced plasma ricinoleic acid in CKD rats.¹⁰
5
6

7 Lysophosphatidic acid (LPA) is a growth factor-like phospholipid. LPA has been known to regulate several
8
9 cellular processes such as cell motility, proliferation, survival and differentiation. It is now recognized as not only
10
11 an intermediate in synthesis of glycerophospholipids but also a mediator in the onset of renal fibrosis.³⁸ Plasma
12
13 LPA(16:0) and LPA(18:2) levels were significantly increased in our CKD patients. This is consistent with our
14
15 previous study which showed significant increase in plasma LPA concentration in CKD compared to the control
16
17 rats.¹⁰ LPA is produced by several enzymes including phospholipases A1/A2, lysophospholipase D/autotaxin,
18
19 glycerol-phosphate acyltransferase, or monoacylglycerolkinase.³⁹ Therefore increased plasma LPA(16:0) and
20
21 LPA(18:2) level in CKD patients may be due to increased expression and/or the activity of these enzymes .
22
23
24
25
26

27 **5. Conclusions**

28
29
30 In summary, we employed a UPLC-HDMS-based metabolomics method to identify a unifying plasma metabolic
31
32 profile in CKD patients and animals with CKDs of distinctly different etiologies. We found a panel of 7 plasma
33
34 metabolites based on the comprehensive screening and validation workflow. These metabolites were significantly
35
36 altered in humans and animals with CKDs of diverse etiologies and as such represent reliable biomarkers of renal
37
38 insufficiency independent of the underlying cause of renal disease.
39
40
41

42 **ASSOCIATED CONTENT**

43 **Supporting Information**

44
45
46 Table S1. Differential plasma metabolites of patients between control and CKD group based on metabolomic
47
48 profile in positive and negative ion modes.
49
50

51
52 Table S2. Differential plasma metabolites of adenine induced CKD rats between control and CKD group based on
53
54 metabolomic profile in positive ion mode and negative ion modes.
55
56

57 Table S3. Differential plasma metabolites of 5/6 nephrectomy induced CKD rats between control and CKD group
58
59

1
2 based on metabolomic profile in positive and negative ion modes.
3

4
5 Figure S1. Multivariate analysis of PCA and PLS-DA.
6

7
8 Figure S2. Heat maps of differential metabolites between control and CKD groups from patients with CKD (A) ,
9
10 adenine induced CKD rats (B) and 5/6 nephrectomy induced CKD rats (C).
11

12
13 Figure S3. Significance analysis for microarrays (SAM) analysis for the important metabolites between CKD and
14
15 Control groups from patients.
16

17 Notes

18
19
20 The authors declare no competing financial interest.
21

22 Acknowledgements

23
24
25 This work was financially supported by the Program for New Century Excellent Talents in University (No.
26
27 NCET-13-0954), the National Natural Science Foundation of China (Nos. J1210063, 81202909 and 81274025)
28
29 and the project “As a Major New Drug to Create a Major National Science and Technology Special” (No.
30
31 2014ZX09304307-02).
32
33
34

35 References

- 36
37 1. Coresh, J.; Selvin, E.; Stevens, L. A.; Manzi, J.; Kusek, J. W.; Eggers, P.; Van Lente, F.; Levey, A. S. Prevalence of
38 chronic kidney disease in the United States. *Jama* **2007**, *298*, 2038-47.
39
40 2. Gansevoort, R. T.; Correa-Rotter, R.; Hemmelgarn, B. R.; Jafar, T. H.; Heerspink, H. J.; Mann, J. F.; Matsushita,
41 K.; Wen, C. P. Chronic kidney disease and cardiovascular risk: epidemiology, mechanisms, and prevention. *Lancet* **2013**,
42 *382*, 339-52.
43
44 3. Tonelli, M.; Wiebe, N.; Culleton, B.; House, A.; Rabbat, C.; Fok, M.; McAlister, F.; Garg, A. X. Chronic kidney
45 disease and mortality risk: a systematic review. *J. Am. Soc. Nephrol.* **2006**, *17*, 2034-47.
46
47 4. Hayek, S. S.; Sever, S.; Ko, Y.-A.; Trachtman, H.; Awad, M.; Wadhvani, S.; Altintas, M. M.; Wei, C.; Hotton, A.
48 L.; French, A. L.; Sperling, L. S.; Lerakis, S.; Quyyumi, A. A.; Reiser, J. Soluble Urokinase Receptor and Chronic
49 Kidney Disease. *N. Engl. J. Med.* **2015**, *373*, 1916-1925.
50
51 5. Nicholson, J. K.; Lindon, J. C.; Holmes, E. 'Metabonomics': understanding the metabolic responses of living
52 systems to pathophysiological stimuli via multivariate statistical analysis of biological NMR spectroscopic data.
53 *Xenobiotica* **1999**, *29*, 1181-9.
54
55 6. Fiehn, O. Metabolomics--the link between genotypes and phenotypes. *Plant Mol Biol* **2002**, *48*, 155-71.
56
57 7. Weiss, R. H.; Kim, K. Metabolomics in the study of kidney diseases. *Nat. Rev. Nephrol.* **2012**, *8*, 22-33.
58
59 8. Zhao, Y. Y.; Cheng, X. L.; Wei, F.; Bai, X.; Tan, X. J.; Lin, R. C.; Mei, Q. Intrarenal metabolomic investigation of
60 chronic kidney disease and its TGF-beta1 mechanism in induced-adenine rats using UPLC Q-TOF/HSMS/MS(E). *J.*

1
2
3
4
5
6
7
8
9
10
11
12
13
14
15
16
17
18
19
20
21
22
23
24
25
26
27
28
29
30
31
32
33
34
35
36
37
38
39
40
41
42
43
44
45
46
47
48
49
50
51
52
53
54
55
56
57
58
59
60

Proteome Res. **2013**, *12*, 692-703.

9. Zhang, Z.-H.; Wei, F.; Vaziri, N. D.; Cheng, X.-L.; Bai, X.; Lin, R.-C.; Zhao, Y.-Y. Metabolomics insights into chronic kidney disease and modulatory effect of rhubarb against tubulointerstitial fibrosis. *Sci. Rep.* **2015**, *5*, 14472.

10. Zhang, Z.-H.; Vaziri, N. D.; Wei, F.; Cheng, X.-L.; Bai, X.; Zhao, Y.-Y. An integrated lipidomics and metabolomics reveal nephroprotective effect and biochemical mechanism of Rheum officinale in chronic renal failure. *Sci. Rep.* **2016**, *6*, 22151.

11. Claramunt, D.; Gil-Pena, H.; Fuente, R.; Hernandez-Frias, O.; Santos, F. Animal models of pediatric chronic kidney disease. Is adenine intake an appropriate model? *Nefrologia* **2015**, *35*, 517-522.

12. Yokozawa, T.; Zheng, P. D.; Oura, H.; Koizumi, F. Animal model of adenine-induced chronic renal failure in rats. *Nephron* **1986**, *44*, 230-4.

13. Vaziri, N. D.; Bai, Y.; Ni, Z.; Quiroz, Y.; Pandian, R.; Rodriguez-Iturbe, B. Intra-renal angiotensin II/AT1 receptor, oxidative stress, inflammation, and progressive injury in renal mass reduction. *J. Pharmacol. Exp. Ther.* **2007**, *323*, 85-93.

14. Zhao, Y. Y.; Feng, Y. L.; Bai, X.; Tan, X. J.; Lin, R. C.; Mei, Q. Ultra performance liquid chromatography-based metabolomic study of therapeutic effect of the surface layer of Poria cocos on adenine-induced chronic kidney disease provides new insight into anti-fibrosis mechanism. *PLoS One* **2013**, *8*, e59617.

15. Choi, J. Y.; Nam, S. A.; Jin, D. C.; Kim, J.; Cha, J. H. Expression and cellular localization of inducible nitric oxide synthase in lipopolysaccharide-treated rat kidneys. *J. Histochem. Cytochem.* **2012**, *60*, 301-15.

16. Jansson, J.; Willing, B.; Lucio, M.; Fekete, A.; Dicksved, J.; Halfvarson, J.; Tysk, C.; Schmitt-Kopplin, P. Metabolomics reveals metabolic biomarkers of Crohn's disease. *PLoS One* **2009**, *4*, e6386.

17. Zhao, Y. Y.; Cheng, X. L.; Wei, F.; Bai, X.; Lin, R. C. Application of faecal metabolomics on an experimental model of tubulointerstitial fibrosis by ultra performance liquid chromatography/high-sensitivity mass spectrometry with MSE data collection technique. *Biomarkers* **2012**, *17*, 721-729.

18. Zhao, Y. Y.; Cheng, X. L.; Cui, J. H.; Yan, X. R.; Wei, F.; Bai, X.; Lin, R. C. Effect of ergosta-4,6,8(14),22-tetraen-3-one (ergone) on adenine-induced chronic renal failure rat: a serum metabolomic study based on ultra performance liquid chromatography/high-sensitivity mass spectrometry coupled with MassLynx i-FIT algorithm. *Clin. Chim. Acta.* **2012**, *413*, 1438-45.

19. Goncalves, A. R.; Fujihara, C. K.; Mattar, A. L.; Malheiros, D. M.; Noronha Ide, L.; de Nucci, G.; Zatz, R. Renal expression of COX-2, ANG II, and AT1 receptor in remnant kidney: strong renoprotection by therapy with losartan and a nonsteroidal anti-inflammatory. *Am. J. Physiol. Renal Physiol.* **2004**, *286*, F945-54.

20. Evans, M.; Bain, S. C.; Hogan, S.; Bilous, R. W. Irbesartan delays progression of nephropathy as measured by estimated glomerular filtration rate: post hoc analysis of the Irbesartan Diabetic Nephropathy Trial. *Nephrol. Dial. Transplant* **2012**, *27*, 2255-63.

21. Coronel, F.; Cigarran, S.; Garcia-Mena, M.; Herrero, J. A.; Calvo, N.; Perez-Flores, I. Irbesartan in hypertensive non-diabetic advanced chronic kidney disease. Comparative study with ACEI. *Nefrologia* **2008**, *28*, 56-60.

22. Zhao, Y. Y.; Cheng, X. L.; Zhang, Y.; Zhao, Y.; Lin, R. C.; Sun, W. J. Simultaneous determination of eight major steroids from Polyporus umbellatus by high-performance liquid chromatography coupled with mass spectrometry detections. *Biomed. Chromatogr.* **2010**, *24*, 222-30.

23. Zhao, Y. Y.; Zhang, L.; Mao, J. R.; Cheng, X. H.; Lin, R. C.; Zhang, Y.; Sun, W. J. Ergosta-4,6,8(14),22-tetraen-3-one isolated from Polyporus umbellatus prevents early renal injury in aristolochic acid-induced nephropathy rats. *J. Pharm. Pharmacol.* **2011**, *63*, 1581-6.

24. Zhao, Y. Y.; Chen, H.; Tian, T.; Chen, D. Q.; Bai, X.; Wei, F. A pharmaco-metabolomic study on chronic kidney disease and therapeutic effect of ergone by UPLC-QTOF/HDMS. *PLoS One* **2014**, *9*, e115467.

25. He, Y. M.; Feng, L.; Huo, D. M.; Yang, Z. H.; Liao, Y. H. Enalapril versus losartan for adults with chronic kidney disease: a systematic review and meta-analysis. *Nephrology (Carlton)* **2013**, *18*, 605-14.

- 1
2
3
4
5
6
7
8
9
10
11
12
13
14
15
16
17
18
19
20
21
22
23
24
25
26
27
28
29
30
31
32
33
34
35
36
37
38
39
40
41
42
43
44
26. Ruiz, S.; Pergola, P. E.; Zager, R. A.; Vaziri, N. D. Targeting the transcription factor Nrf2 to ameliorate oxidative stress and inflammation in chronic kidney disease. *Kidney Int.* **2013**, *83*, 1029-41.
27. Lee, B. H.; Hsu, W. H.; Chang, Y. Y.; Kuo, H. F.; Hsu, Y. W.; Pan, T. M. Ankaflavin: a natural novel PPARgamma agonist upregulates Nrf2 to attenuate methylglyoxal-induced diabetes in vivo. *Free Radic. Biol. Med.* **2012**, *53*, 2008-16.
28. Li, H.; Zhang, L.; Wang, F.; Shi, Y.; Ren, Y.; Liu, Q.; Cao, Y.; Duan, H. Attenuation of glomerular injury in diabetic mice with tert-butylhydroquinone through nuclear factor erythroid 2-related factor 2-dependent antioxidant gene activation. *Am. J. Nephrol.* **2011**, *33*, 289-97.
29. Aminzadeh, M. A.; Reisman, S. A.; Vaziri, N. D.; Khazaeli, M.; Yuan, J.; Meyer, C. J. The synthetic triterpenoid RTA dh404 (CDDO-dhTFFA) restores Nrf2 activity and attenuates oxidative stress, inflammation, and fibrosis in rats with chronic kidney disease. *Xenobiotica* **2014**, *44*, 570-8.
30. Mutsaers, H. A.; Engelke, U. F.; Wilmer, M. J.; Wetzels, J. F.; Wevers, R. A.; van den Heuvel, L. P.; Hoenderop, J. G.; Masereeuw, R. Optimized metabolomic approach to identify uremic solutes in plasma of stage 3-4 chronic kidney disease patients. *PLoS One* **2013**, *8*, e71199.
31. Choi, J. Y.; Yoon, Y. J.; Choi, H. J.; Park, S. H.; Kim, C. D.; Kim, I. S.; Kwon, T. H.; Do, J. Y.; Kim, S. H.; Ryu do, H.; Hwang, G. S.; Kim, Y. L. Dialysis modality-dependent changes in serum metabolites: accumulation of inosine and hypoxanthine in patients on haemodialysis. *Nephrol. Dial. Transplant* **2011**, *26*, 1304-13.
32. Graham, K. A.; Reaich, D.; Channon, S. M.; Downie, S.; Goodship, T. H. Correction of acidosis in hemodialysis decreases whole-body protein degradation. *J. Am. Soc. Nephrol.* **1997**, *8*, 632-7.
33. Duranton, F.; Cohen, G.; De Smet, R.; Rodriguez, M.; Jankowski, J.; Vanholder, R.; Argiles, A. Normal and pathologic concentrations of uremic toxins. *J. Am. Soc. Nephrol.* **2012**, *23*, 1258-70.
34. Allison, S. J. Fibrosis: dysfunctional fatty acid oxidation in renal fibrosis. *Nat. Rev. Nephrol.* **2015**, *11*, 64.
35. Shearer, G. C.; Carrero, J. J.; Heimbürger, O.; Barany, P.; Stenvinkel, P. Plasma fatty acids in chronic kidney disease: nervonic acid predicts mortality. *J. Ren. Nutr.* **2012**, *22*, 277-83.
36. Vaziri, N. D. Lipotoxicity and impaired high density lipoprotein-mediated reverse cholesterol transport in chronic kidney disease. *J. Ren. Nutr.* **2010**, *20*, S35-43.
37. Vaziri, N. D. HDL abnormalities in nephrotic syndrome and chronic kidney disease. *Nat. Rev. Nephrol.* **2016**, *12*, 37-47.
38. Pradere, J. P.; Gonzalez, J.; Klein, J.; Valet, P.; Gres, S.; Salant, D.; Bascands, J. L.; Saulnier-Blache, J. S.; Schanstra, J. P. Lysophosphatidic acid and renal fibrosis. *Biochim Biophys Acta* **2008**, *1781*, 582-7.
39. Moolenaar, W. H.; van Meeteren, L. A.; Giepmans, B. N. The ins and outs of lysophosphatidic acid signaling. *Bioessays* **2004**, *26*, 870-81.

45 Table 1. Summary of clinical and demographic baseline characteristics of patients with CKD and healthy control
46
47 subjects in this study

	Control	Patients with CKD
Age (years)	53.5±12.5	55.3±13.2
Body mass index (kg/m ²)	23.6±3.2	24.8±4.7
SBP (mm Hg)	122.4±13.4	143.3±14.3***
DBP (mm Hg)	76.4±10.2	83.5±13.4***

eGFR (ml/min/1.73m ²)	98.9±16.4	15.4±4.8***
Urea (mmol/L)	2.61±0.56	17.1±7.8***
Plasma creatinine (μmol/L)	66.9±15.2	4.98±1.95***
Triglycerides (mmol/L)	1.61±0.54	1.91±0.69**
Total cholesterol(mmol/L)	4.91±1.31	4.97±1.39
Urine proteins (g/24h)	-	1.87±1.47***
Uric acid (μmol/L)	298.3±85.4	470±129***
Albumin (g/L)	47.±8.1	34.9±5.9***
White blood cell (×10 ⁹ /L)	6.61±2.04	8.94±2.91***
Red blood cell (×10 ¹² /L)	4.48±1.45	3.02±0.98***
Haemoglobin (g/L)	143.2±13.5	98.5±24.6***

Results are expressed as the means±standard deviation, ***P*<0.01, ****P*<0.001 compared with healthy control group.

Table 2. Biochemical parameters in adenine-induced CKD rats and 5/6 nephrectomized rats.

Biochemical parameters	Adenine-induced CKD model at 6 week		5/6 nephrectomy-induced CKD model at 12 week	
	Control	CKD	Control	CKD
serum creatinine (μmol/L)	42.6±1.91	92.3±6.03**	41.2±5.20	71.2±5.52**
Urea (mmol/L)	6.92±0.88	18.82±0.97**	19.19±0.62	40.95±1.71**
Ccr (ml/min/kg)	7.35 ± 0.69	1.26 ± 0.24**	5.52±0.51	1.74±0.19**
Triglycerides (mmol/L)	0.53±0.14	0.92±0.31**	0.51±0.08	1.13±0.02**
Total cholesterol (mmol/L)	1.17±0.14	2.01±0.52**	1.83±0.11	5.73±0.27**

Values are means ± SE (n = 8 in each group). Ccr, creatinine clearance; **p* < 0.05, ***p* < 0.01 compared to control group.

Table 3. Physiologic parameters of animals.

Adenine model	CTL	Model	ergone treatment	IBR treatment
Body weight (g)	329.3±16.4	276.5±28.5**	277.1±30.1	314±42.9
Kidney weight index (g/g×100)	0.85±0.07	4.08±0.62**	3.35±0.52 [^]	2.13±0.65 ^{^^}

Liver weight index (g/g×100)	3.49±0.45	3.28±0.57	3.14±0.51	3.33±0.65
Food (g/100g BW)	20.4±5.5	19.4±8.7	18.5±7.4	22.3±8.8
Water (g/100g BW)	25.9±6.9	29.2±7.9	30.5±6.1	27.5±5.7
5/6 nephrectomy model	CTL	Model	Enalapril treatment	RTA dh404 treatment
Body weight (g)	396.1±25.4	367.2±31.6	387.7±37.5	374.5±34.5
Kidney weight index (g/g×100)	0.87±0.13	0.35±0.07**	0.39±0.10	0.37±0.09
Liver weight index (g/g×100)	3.85±0.52	3.65±0.61	3.75±0.56	3.73±0.49
Food (g/100g BW)	18.7±5.6	19.5±6.6	17.4±6.8	20.1±5.4
Water (g/100g BW)	26.4±7.4	28.5±7.5	25.8±7.1	24.6±5.9

Results are expressed as the means±standard deviation, *p< 0.05, **p< 0.01 compared to control group; ^p< 0.05,

^^p< 0.01 compared to CKD group.

Table 4. ROC Analysis Results for 17 candidate biomarkers from patients with CKD.

metabolites	ESI	m/z	MS ^E	losses	d.value	AUC	standard error	95% CI lower	95% CI upper	sensitivity	specificity
12-Ketodeoxycholic acid ^b	-	389.2707	371.2225	-H ₂ O	-21.963	1.000	0.001	0.963	1.000	0.98	1.00
Hypotaurine ^a	+	110.0277	92.0176	-H ₂ O	20.474	0.995	0.004	0.955	1.000	0.94	1.00
LPA(16:0) ^c	+	433.2324	313.2748	-H ₃ PO ₄	-12.180	0.994	0.005	0.952	1.000	0.96	0.98
			239.2393	-C ₃ H ₇ O ₆ P							
3-Methylhistidine ^b	+	170.0929	126.1051	-CO ₂	-9.132	0.988	0.009	0.943	1.000	0.98	0.98
			109.0779	-NH ₃							
Argininic acid ^a	+	176.1072	132.1095	-CO ₂	-13.588	0.987	0.007	0.940	0.999	0.94	0.96
Indolelactic acid ^b	+	206.0815	188.0333	-H ₂ O	-8.139	0.960	0.017	0.900	0.989	0.86	0.92
LPA(18:2) ^c	-	433.2344	336.6553	-H ₃ PO ₄	-9.515	0.960	0.017	0.901	0.989	0.92	0.90
			262.9866	-C ₃ H ₇ O ₆ P							
Stearic acid ^c	+	285.2781	241.2849	-CO ₂	10.652	0.938	0.026	0.871	0.976	0.94	0.90
Cytosine ^a	+	112.0496	—	—	10.113	0.935	0.023	0.868	0.975	0.94	0.80
Ricinoleic acid ^c	-	297.2423	253.2491	-CO ₂	8.726	0.908	0.031	0.834	0.957	0.84	0.92
3-hydroxyhexadecanoic acid ^c	+	273.2429	229.2496	-CO ₂	8.038	0.895	0.034	0.817	0.947	0.80	0.92
MG(15:0) ^c	-	315.2528	224.5494	-C ₃ H ₇ O ₃	-6.757	0.889	0.038	0.810	0.943	0.98	0.80
Lipoyllysine ^b	+	335.1514	318.1251	-NH ₃	8.285	0.879	0.034	0.799	0.936	0.82	0.80
Arachidic acid ^c	+	313.3008	269.3076	-CO ₂	7.403	0.877	0.036	0.796	0.934	0.80	0.86

Creatinine ^a	+	114.0669	—	—	-7.093	0.846	0.039	0.760	0.910	0.74	0.84
Tryptophano ^b	+	184.0714	166.0232	-H ₂ O	-6.764	0.846	0.042	0.760	0.910	0.78	0.86
Docosapentaenoic acid ^c	+	348.2888	304.2956	-CO ₂	6.790	0.837	0.042	0.750	0.903	0.68	0.90

Based on their AUC values, these metabolic biomarkers are sorted in descending order. ^aMetabolites validated with authentic chemicals. ^bMetabolites validated with their analogue structure of authentic chemicals. ^cMetabolites were predicted according to the MS and MS/MS.

Figure 1. Overview of study design. Human plasma samples in each phase were obtained from independent patient and control cohorts.

Figure 2. A. Venn diagram of the significantly different metabolites from patients, adenine model rats, and 5/6 nephrectomy rats when the models and the controls were compared. B. The z-score plot for the comparison between control patients (blue) and CKD patients (red). Each point represents one metabolite in one sample. C. Heat maps of 36 candidate biomarkers between control and CKD groups from patients with CKD. Rows: metabolites; Columns: samples. D. Receiver operating characteristic (ROC) curve of 17 candidate biomarkers from patients with CKD in discovery phase. OCTLB4: Omega-Carboxy-trinor-leukotriene B4.

Figure 3. Box-and-whisker plots showing significant differential metabolite changes in plasma between control and CKD groups. Boxes show interquartile ranges, lines show medians and whiskers extend to extreme data points within 1.5 times interquartile range. Diamond represented metabolite intensity in plasma samples. Green and red represent control and CKD, respectively. * $P < 0.05$; ** $P < 0.01$; *** $P < 0.001$ compared with the control group.

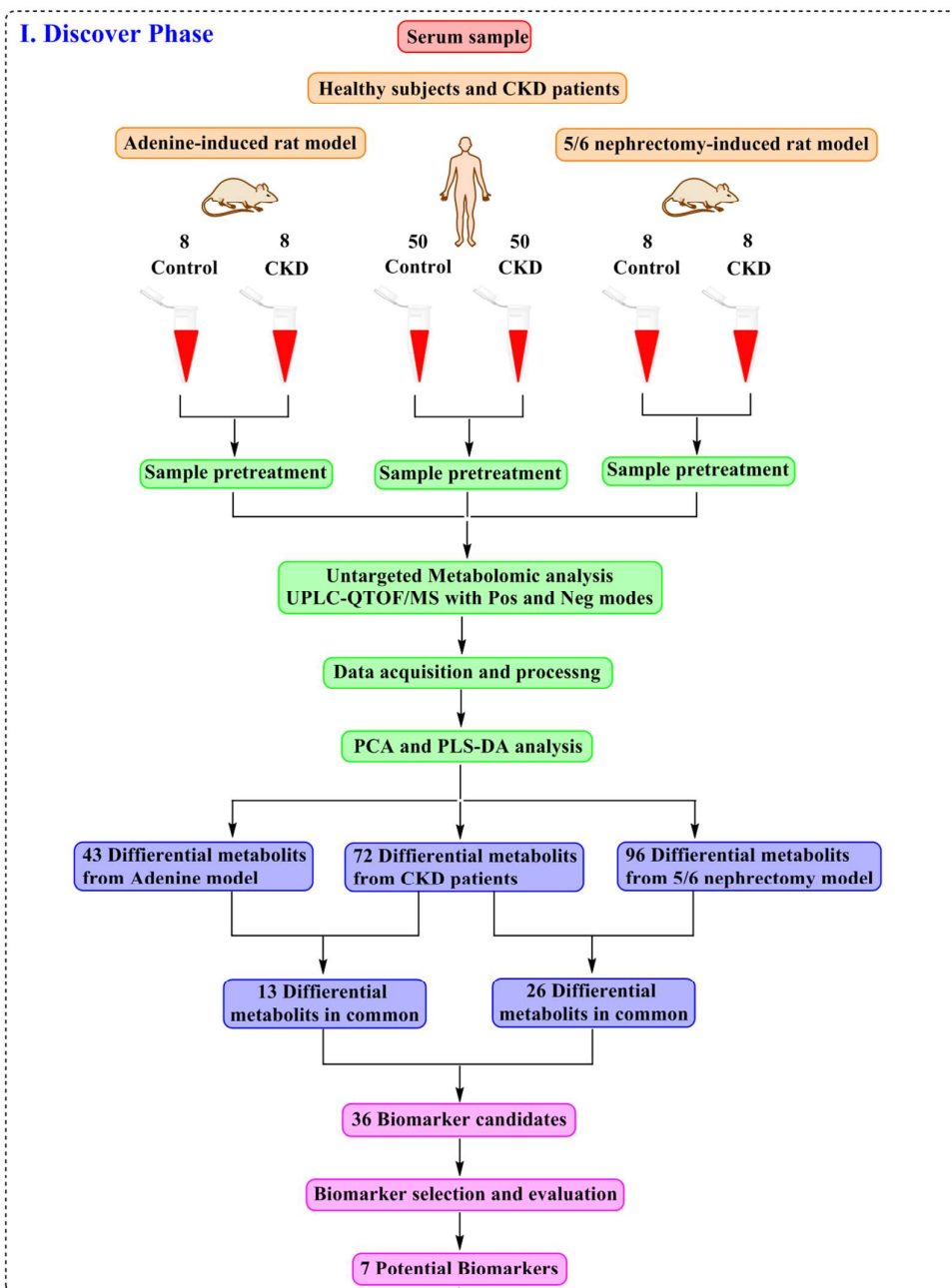
1
2
3 Figure 4. (A) Hierarchical clustering of biomarkers. Correlation analysis of the 7 candidate biomarkers between
4 control and CKD groups in the samples of patients. (B) Diagnostic performances of the 7 candidate biomarkers in
5 plasma based on the PLS-DA model. The black dots and black circles with red squares are for the incorrectly
6 predicted samples in patients with CKD and controls, respectively. (C) ROC curves of the individual biomarkers
7 from patients with CKD in validation phase. (D) ROC curves of the combination of the 7 biomarkers from
8 patients with CKD in validation phase. (E) Representative photomicrographs of the H&E staining, Masson
9 trichrome staining, TGF- β 1 and ED-1 immunohistochemistry of kidney sections from control, CKD,
10 CKD+irbesartan and CKD+ergone rats in adenine model. (F) Plasma creatinine (CREA) and urea levels of the
11 control, CKD, CKD+irbesartan and CKD+ergone rats in adenine model. (G) Relative concentrations of biomarker
12 candidates in the control, CKD, CKD+irbesartan and CKD+ergone rats in adenine model. (H) Representative
13 photomicrographs of the H&E, PAS staining, PCNA and iNOS immunohistochemistry of kidney sections from
14 control, CKD, CKD+enalapril and CKD+RTA dh404 rats in 5/6 nephrectomy model. (I) CREA and urine protein
15 levels of the control, CKD, CKD+enalapril and CKD+RTA dh404 rats in 5/6 nephrectomy model. (J) Relative
16 concentrations of biomarker candidates in the control, CKD, CKD+enalapril and CKD+RTA dh404 rats in 5/6
17 nephrectomy model. (K) Renal fibrotic protein expression in adenine model. Expression levels of TGF- β 1 and
18 ED-1 proteins were determined in control, CKD, CKD+irbesartan and CKD+ergone rats by Western blot analysis.
19 GAPDH served as the loading control. (L) Renal fibrotic protein expression in 5/6 nephrectomy model.
20 Expression levels of PCNA and iNOS proteins were determined in control, CKD, CKD+enalapril and CKD+RTA
21 dh404 rats by Western blot analysis. GAPDH served as the loading control. (M) Relative concentrations of the
22 biomarker candidates in the control subjects, CKD, CKD+enalapril and CKD+irbesartan patients. * $p < 0.05$, ** $p <$
23 0.01 , *** $p < 0.001$ compared to control group; $\wedge p < 0.05$, $\wedge\wedge p < 0.01$, $\wedge\wedge\wedge p < 0.001$ compared to CKD group.
24
25
26
27
28
29
30
31
32
33
34
35
36
37
38
39
40
41
42
43
44
45
46
47
48
49
50
51
52
53
54
55
56
57
58
59
60

Figure 5. Pathway analysis of the identified metabolites. (A) Pathway analysis of 36 biomarker candidates. Small

1
2 p value and big pathway impact factor indicate that the pathway is greatly influenced. (B) Metabolic pathway of
3
4 identified biomarkers. Red color represents increased metabolites in CKD group; Blue color represents decreased
5
6 metabolites in CKD group. Dotted arrow indicates multiple processes. The solid arrow indicates a single process.
7
8
9
10
11
12
13
14
15
16
17
18
19
20
21
22
23
24
25
26
27
28
29
30
31
32
33
34
35
36
37
38
39
40
41
42
43
44
45
46
47
48
49
50
51
52
53
54
55
56
57
58
59
60

Figure 1

I. Discover Phase



II. Validation Phase

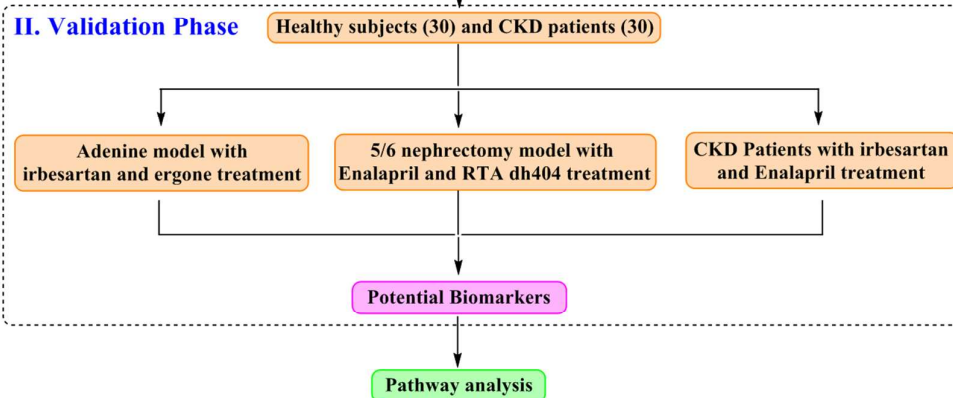


Figure 2

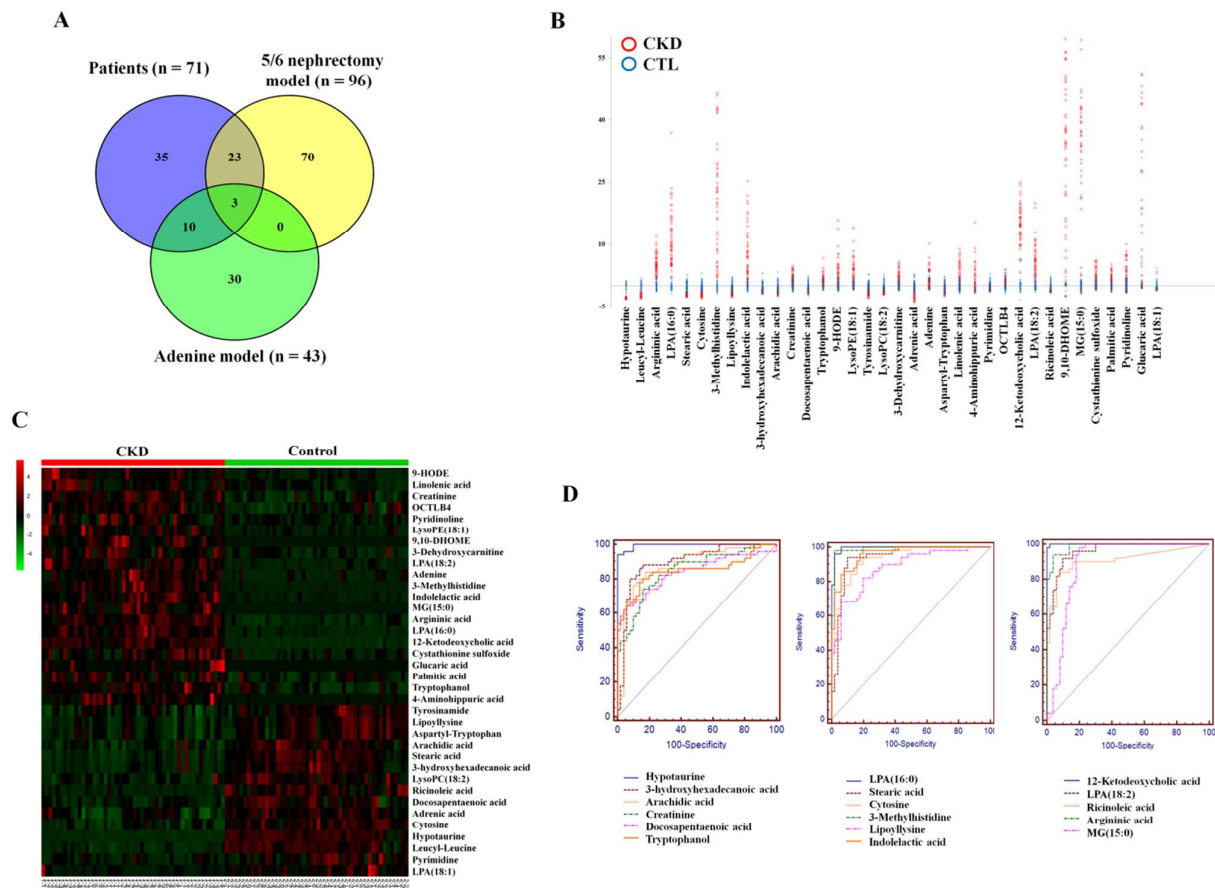


Figure 3

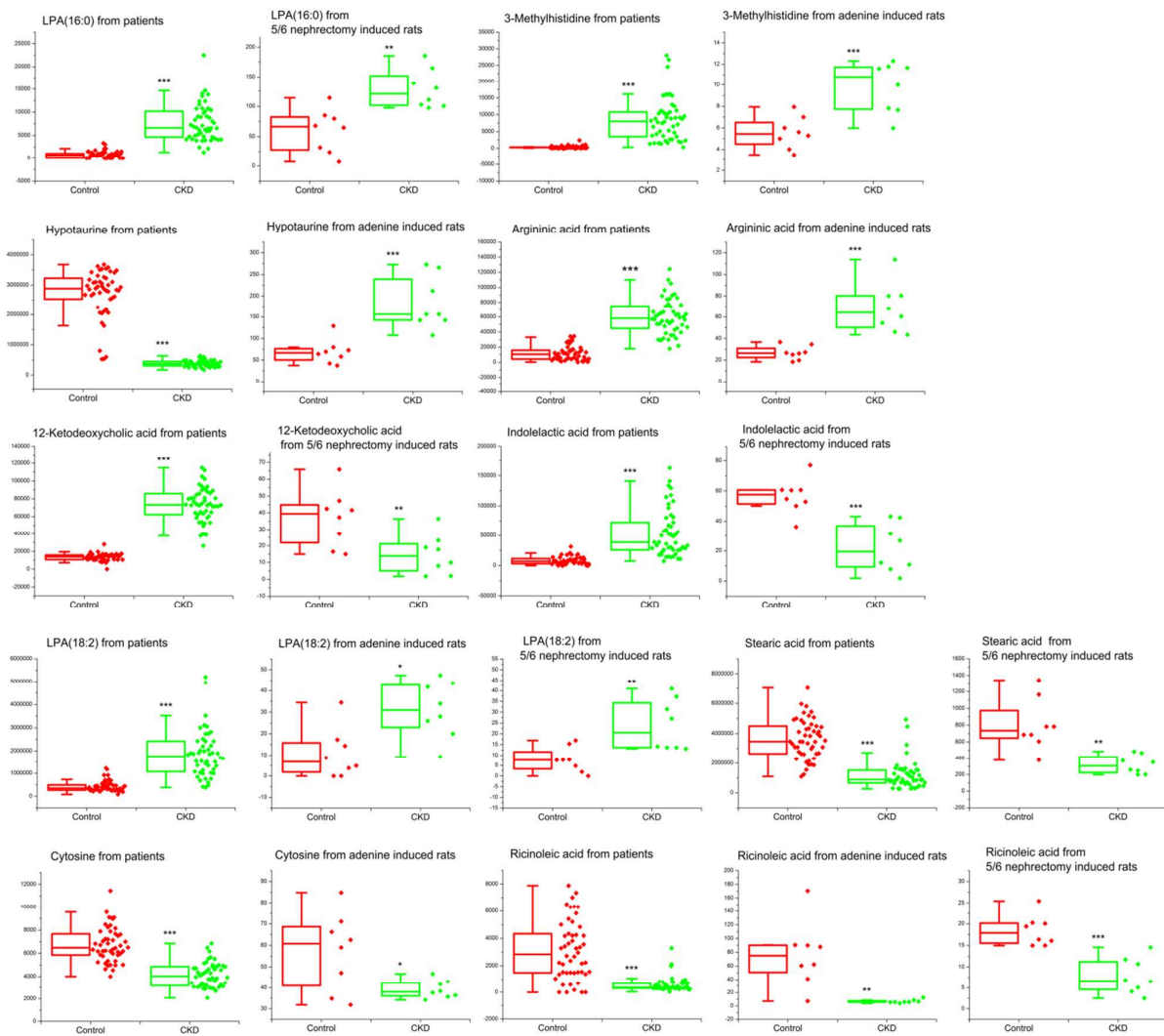


Figure 4

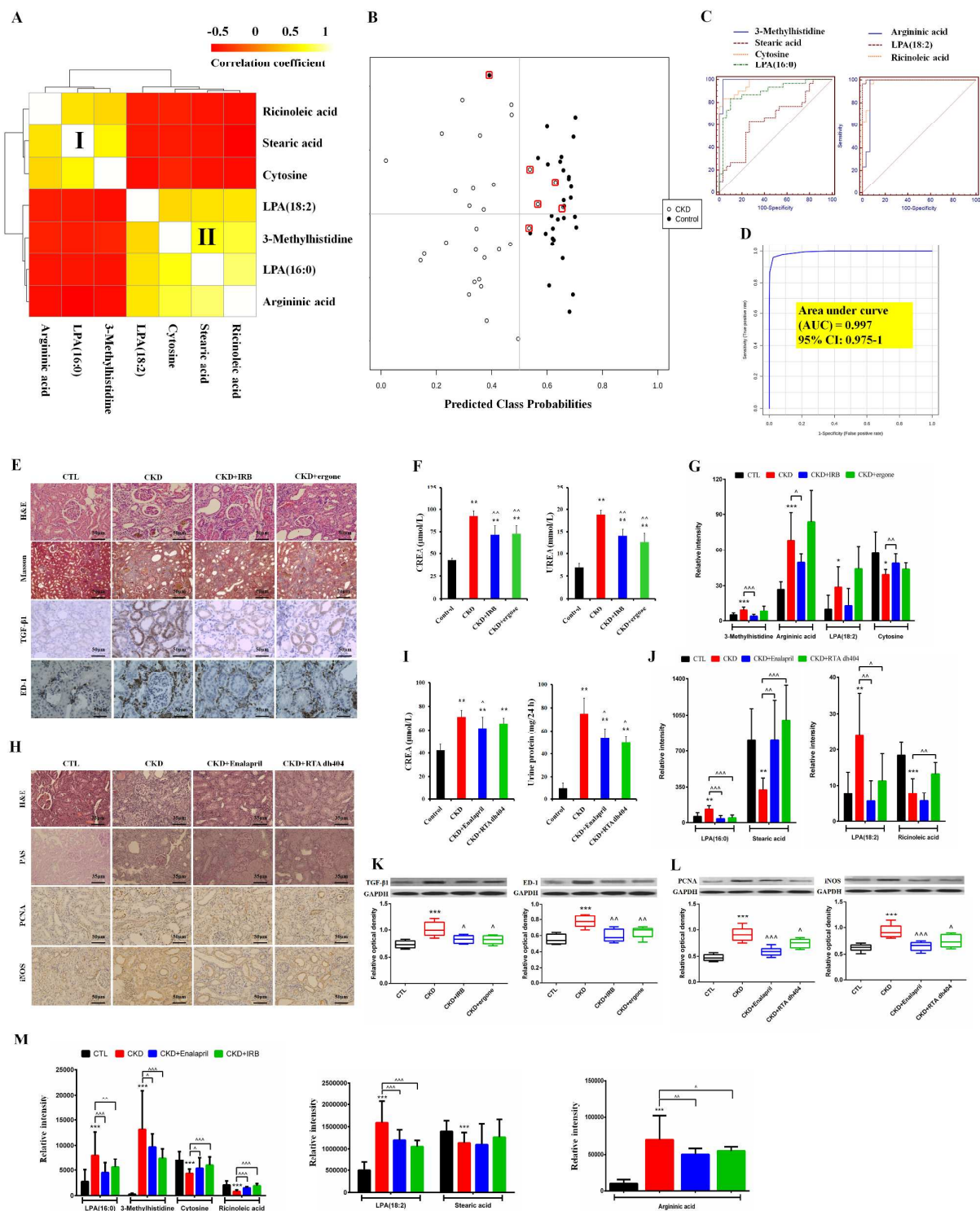
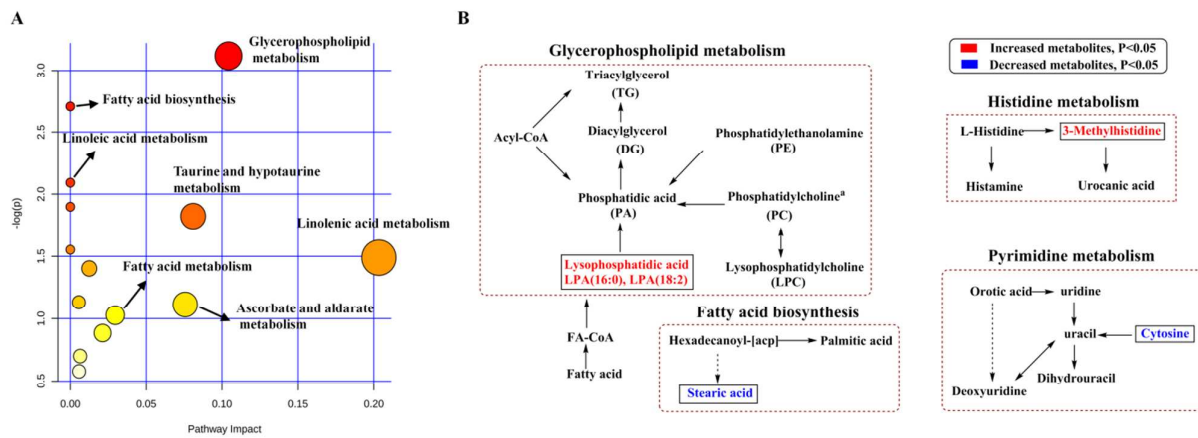


Figure 5



For TOC only

